GEM*: A Molecular Electronic Density-Based Force Field for Molecular Dynamics Simulations

Robert E. Duke,[†] Oleg N. Starovoytov,[†] Jean-Philip Piquemal,[‡,§] and G. Andrés Cisneros*,[†]

[†]Department of Chemistry, Wayne State University, Detroit, Michigan 48202, United States

[‡]Sorbonne Universités, UPMC Univ Paris 06, UMR 7616 Laboratoire de Chimie Théorique case courrier 137, 4 place Jussieu 75005, Paris, France

[§]CNRS, UMR 7616 Laboratoire de Chimie Théorique case courrier 137, 4 place Jussieu 75005, Paris, France

S *Supporting Information*

ABSTRACT: GEM*, a force field that combines Coulomb and Exchange terms calculated with Hermite Gaussians with the polarization, bonded, and modified van der Waals terms from AMOEBA is presented. GEM* is tested on an initial water model fitted at the same level as AMOEBA. The integrals required for the evaluation of the intermolecular Coulomb interactions are efficiently evaluated by means of reciprocal space methods. The GEM* water model is tested by comparing energies and forces for a series of water oligomers and MD simulations. Timings for GEM* compared to AMOEBA are presented and discussed.
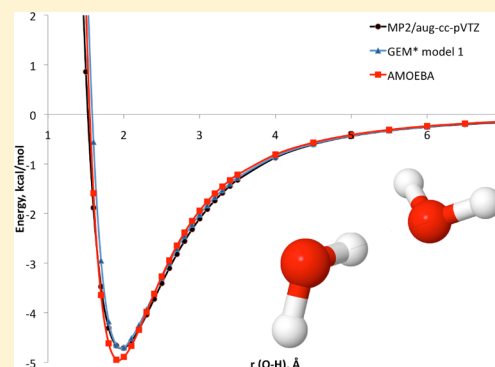
The development of force fields to simulate chemical and biochemical systems by classical molecular dynamics simulations is a field of intense research.[1-6] Most of these force fields calculate the properties of the systems by separating the energy (and forces) into bonded and nonbonded contributions. The intermolecular interactions are calculated by means of an explicit Coulomb term and a function (e.g., Lennard–Jones, Buckingham, or buffered Halgren) that evaluates the van der Waals interactions. In general, the Coulomb term is computed by atom centered point charges. One problem with this approximation is the result of a loss in accuracy because of the loss of charge density anisotropy and the failure to account for penetration effects.[7]

Several force fields, such as AMOEBA, SIBFA, EFP, X-Pol, NEMO, etc. that employ distributed multipoles and use explicit polarization, have been proposed.[8-14] The use of distributed multipoles provides a better description of the charge density anisotropy and results in an improved treatment of electrostatics.[7,15-19] However, multipoles still suffer from charge penetration errors at close range.[7,20] This issue may be ameliorated by the use of damping functions to correct the electrostatic interactions at close distances.[20-25]

Another possibility to avoid the charge penetration and anisotropy shortcomings is to employ a continuous description of the molecular charge density. Several methods that describe the electronic distribution explicitly have been proposed.[26-33] Some of us have previously introduced the Gaussian Electrostatic Model (GEM).[34-36] GEM uses the density fitting (DF) formalism[37-39] to expand the molecular density using Hermite Gaussian auxiliary basis sets (ABSs).

Molecules in the GEM formalism are fitted to reproduce gas phase *ab initio* QM intermolecular interaction results from energy decomposition analysis (EDA).[40-49] The fitted densities are used to calculate each of the components of the QM intermolecular interaction (Coulomb, exchange–repulsion, polarization, charge–transfer, and dispersion). The use of continuous functions provides a more accurate description of molecular properties compared to conventional point charges.[36] We have also shown that GEM results in very accurate energies and forces for a range of systems including homodimers, heterodimers, and molecular clusters, and it can be used in multiscale implementations.[35,36,50,51] However, molecular dynamics simulations using GEM had been impractical due to the lack of an analytic form for the gradient of the charge–transfer term.

The use of Hermite Gaussians results in the need to evaluate a large number of Coulomb and overlap integrals. In order to efficiently evaluate these integrals, we have extended the smooth particle mesh Ewald (PME)[52] and fast Fourier Poisson (FFP)[53] methods to allow the evaluation of continuous Gaussian functions under periodic boundary conditions.[36,54]

In this contribution, we present an intermediate step to enable the use of GEM for MD calculations. To this end, we have developed a force field that we call GEM*, which combines the Coulomb and exchange–repulsion terms from GEM with the polarization, (modified/reparametrized) van der

Waals and bonded terms from AMOEBA. This new force field has been implemented in a modified version of pmemd in the AMBER suite of programs. As a test case, we present the parametrization of GEM* for a model of water based on the original AMOEBA model.[10,55−57]

For our initial water model, the total intermolecular energies were parametrized to reproduce QM reference data only. Briefly (see Supporting Information for detailed descriptions), the Coulomb interaction is calculated by using the frozen fitted GEM* densities to calculate electron−electron and electron−nuclear Coulomb interactions and added to the nuclear−nuclear interactions.[36] The exchange component is determined by the Wheatley−Price overlap model[58,59] by calculating the charge density overlap with the GEM* densities.[35,36] The polarization is calculated by the AMOEBA model using inducible point dipoles damped at short-range using a Tholè function.[55,60] The last nonbonded term is a modified buffered Halgren function that only represents the dispersion component (see Supporting Information). Finally, the bonded terms are the same as in the original AMOEBA model.

The fitting procedure is carried out in several stages by using energy decomposition analysis (EDA) data and total intermolecular energies corrected for basis set superposition error (BSSE; see Supporting Information). The Coulomb intermolecular interactions were calculated at the MP2/aug-cc-pVTZ level by using frozen QM densities with an in-house FORTRAN90 program. The exchange−repulsion and polarization terms were obtained using the restricted variational space (RVS)[42] method as implemented in GAMESS at the HF/aug-cc-pVTZ level. In the first step, the GEM* coefficients for the density were obtained by minimizing the error of the Coulomb interaction with respect to the Coulomb EDA reference. Subsequently, the exchange factor was obtained by a linear regression to RVS dimer data over the range of 1.7−3 Å. This was followed by the polarization, which was also matched to its RVS counterpart. In this case, the multipoles employed to calculate the permanent electric fields were obtained from the GEM* fitted densities as previously described.[61] The Tholè parameter for the damping of the induced damping was reduced to 0.35 to better reproduce the polarization interaction. Finally, the modified Halgren term was fitted to reproduce the difference of the BSSE corrected total intermolecular interaction and each of these terms. That is, $E_{VdW} = E_{MP2(BSSE)} - E_{Coulomb}^{GEM*} - E_{exchange-repulsion}^{GEM*} - E_{polarization}^{GEM*}$.

To show the ability of GEM* to reproduce intermolecular interactions for water, we compared total energies calculated with GEM* to QM reference values corrected for basis set superposition error via the counterpoise method for a series of water dimers and clusters up to hexamer. The reference data were calculated at the MP2(full)/aug-cc-pVTZ level to match the original AMOEBA parametrization.[10,55−57] The molecular electronic density used to obtain the fitting coefficients for GEM* was calculated at the same level of theory as above for a water molecule at the AMOEBA equilibrium geometry.

Two ABSs were tested, A1 and A2,[62,63] that comprise 42 and 70 basis functions per water monomer, respectively. For consistency, the corresponding distributed multipoles for each ABS were matched to the Hermite Gaussians for the calculation of the electric fields required for the polarization. The multipoles for the A1 ABS have been previously reported in ref 61, the multipoles for the A2 ABS are given in the Supporting Information. As noted previously in ref 61, the A1 ABS only involves s-type functions on hydrogen atoms, which

results in only point charges. The slightly bigger A2 ABS includes one spd-type shell on hydrogens, which gives rise to distributed dipoles and quadrupoles on these atoms. This results in different magnitudes for the charges. The original multipoles obtained with the A1 ABS result in monopoles of −0.93 on O and +0.465 on each H.[61] Conversely, the A2 derived monopoles correspond to −0.414 and +0.207 on O and H, respectively. The monopoles obtained from the A2 ABS are closer to the values obtained with GDMA for the original AMOEBA model.[64,55]

Three different parametrizations have been explored, which we term models 1−3 in the discussion below (see Supporting Information for details). Briefly, model 1 uses the A2 ABS and was fitted to reproduce intermolecular interaction energies for the canonical water dimer (see Figure 1), several random
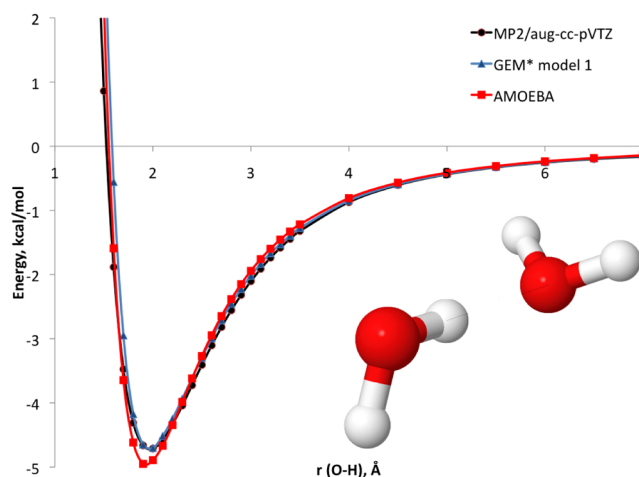

Figure 1. Total intermolecular interaction energy for the canonical water dimer.

dimers, and selected water clusters from ref 65. Models 2 and 3 were parametrized to reproduce intermolecular energies for the canonical water dimer only using the A2 (model 2) and A1 (model 3) ABSs. All calculations for GEM* for intermolecular interactions and MD were performed with a modified pmemd version in the AMOEBA suite of programs.[1]

Models 2 and 3 were observed to reproduce the total intermolecular interaction (as well as the separate components) with respect to the corresponding QM reference energies for the canonical water dimer very well. However, the atomic forces with model 3 show deviations in some cases such as the force in the X direction for one of the O atoms (see Supporting Information). This is due to the small size of the A1 ABS, which is not able to reproduce the atomic forces. In the case of the A2 ABS, the calculated atomic forces are in good agreement with the QM reference.

Significant deviations were observed when the GEM* model 2 and model 3 parameters were employed to calculate the intermolecular energy of the random dimers or the binding energy for the clusters (see Supporting Information). For example, in the case of the energies for the random dimers calculated with both of these models, the mean unsigned errors (maximum absolute error) are 0.20 (1.36) and 0.25 (1.41) kcal/mol for model 2 and model 3, respectively. It was also observed that the many-body effects were not captured by these parametrizations since the binding energy errors for the water

hexamers were 2−3 kcal/mol for model 2 in most cases (see Supporting Information).

The reason for these large differences is due to the poor description of the H−H interactions. Indeed, for most random dimers where only heteroatoms interact directly (O−H, e.g., hydrogen bonds) the errors were well below 0.1 kcal/mol. However, for four dimers where the monomers are oriented such that the H atoms interact directly, the errors are significant. This problem is also the reason why model 2 gives large deviations in the binding energy for larger clusters.

In contrast, all results for model 1 showed good agreement with the QM references for dimers as well as larger clusters. In the case of the random dimers, the mean unsigned error and maximum absolute error for the A2 model are 0.04 and 0.34 kcal/mol, respectively, compared to 0.02 and 0.57 kcal/mol for AMOEBA. In the case of the binding energy for the water clusters, the mean absolute error for GEM* model 1 is 1.43 kcal/mol compared to 1.60 kcal/mol with AMOEBA. Interestingly, the maximum absolute error for GEM* model 1 is larger at 3.19 kcal/mol than the AMOEBA maximum absolute error of 2.67 kcal/mol. This large error corresponds to the water hexamer in the prism configuration. However, with that exception, all other pentamers and hexamers tested showed smaller errors in binding energy with GEM* model 1 (see Supporting Information).

These results show that a relatively better parametrization was obtained once a slightly larger data set that included different dimer orientations was considered. Recently, Babin et al. have developed a novel water model parametrized only from QM data[66,67] using results from 40 000 dimers calculated at the CCSD/CBS level. In a future contribution, we will present results that employ the data set developed by Babin et al. for our parametrization. For the purposes of determining the feasibility and performance of MD simulations with GEM*, the model 1 parameters were deemed to be sufficiently accurate.

To determine the feasibility and performance of GEM*, we carried out NVE simulations on several water boxes (216, 512, 1024, 2048, and 4096 molecules). The initial GEM* implementation is only serial, and all tests were carried out on a Xeon X5550 (Nehalem) CPU with 12 GB of memory. All MD simulations were carried out at 300 K with an 8 Å cutoff for van der Waals interactions, using the Beeman integrator, a 1 fs time step, and a dipole tolerance for the SCF convergence of 10^{-6}. The calculation of the polarization with the induced dipoles was performed using the PME method.

As mentioned above and described in detail in refs 36 and 54, the Coulomb and overlap integrals can be efficiently evaluated using reciprocal space methods. This is achieved by separating the total density of each monomer into compact and diffuse contributions. On the basis of this separation, all compact−compact interactions can be evaluated in direct space and all compact−diffuse and diffuse−diffuse integrals may be determined in reciprocal space.[36,54] The current GEM* implementation includes PME, FFP, and Ewald[68] for the integral calculations. In practice, the overlap integrals for both A1 and A2 tend to 0 at distances around 6 Å. Therefore, only the Coulomb interactions were calculated using the reciprocal space methods. For the exchange, all integrals were evaluated in direct space exclusively using the same cutoff as for the van der Waals interactions.

To test the performance of this initial code (which has not been optimized or tuned), we carried out 100 MD steps of NVE simulations on the five water boxes. In all cases, the systems were replicated periodically. Timings for all the tested systems are shown in Table 1. For comparison, we performed

Table 1. Timings for Different Water Boxes with GEM* Model 1 (All Times in Seconds)

number of waters	all compact	PME with 2 diffuse hermites	FFP with 2 diffuse hermites
216	100.04	127.12[a,b]	266.84[a]
512	220.86	239.70[a,b]	373.48[a]
1024	457.99	495.29[a,b]	682.31[a]
2048	1172.43	1177.05[a,b]	1368.90[a]
4096	3319.59	3197.51[c]	4180.62[d]

[a]FFT grid = 84^3. [b]B-spline order = 10. [c]FFT grid = 92^3, B-spline order = 12. [d]FFT grid = 100.

the calculations for all cases with the Coulomb integrals evaluated completely in direct space (all Gaussians set as compact) or by placing two Gaussians from the A2 ABS (see Supporting Information) in the diffuse set and using PME or FFP. As discussed previously, the evaluation of the Hermite Gaussians in reciprocal space requires significantly larger grids and b-spline orders (see Table 1 for values).[36,54] In the case of the three smallest boxes, the calculations are faster when all the integrals are evaluated in direct space. The crossover to a faster calculation with PME happens with the 2048 or 4096 box. This is due to the large overhead for the FFTs due to the fine grids required for accurate evaluation of the energies and forces in reciprocal space.

In the present implementation, the smallest (216) water box takes 100 s for the 100 MD steps compared to 8 s for AMOEBA in the same code-base/CPU. However, note that for this smallest box, each MD step involves the energy/force calculation of all GEM* terms including the evaluation of Coulomb and overlap integrals for 15 120 basis functions. That is, our code is able to evaluate all of these integrals for a single step in 1 s. For the 4096 box, the full system comprises 286 720 basis functions. Moreover, there are still significant time savings that can be obtained by careful tuning of the PME/FFP parameters, optimization of the code, as well as parallelization.

To test the stability of the force field, the 216 water box was subjected to an NVE simulation for over 400 ps. The system was observed to conserve energy over the entire simulation period (see Supporting Information). Radial distribution functions for O−O, O−H, and H−H were calculated from this simulation and compared to those calculated with the original AMOEBA model and experimental curves from neutron scattering data[69] (see Figure 2). It is observed that the rdf's for O−H and H−H are very similar to the AMOEBA and experimental results. In the case of the O−O rdf, the first and third peaks agree with both experimental results and AMOEBA. However, the second peak is not as pronounced, indicating that the second solvation shell is not as well structured in the current parametrization.

The heat of vaporization can be calculated from the difference in potential energies between the liquid and gas phases. The average potential energy of the gas, 0.9 kcal/mol, is the same as determined previously.[61] The average potential energy is 8.57 (8.91) kcal/mol, resulting in a calculated heat of vaporization of 10.07 (10.41) kcal/mol for model 1 (model 2). The calculated heat of vaporization for model 1 has an error of 4.2% compared to the experimental value of 10.51 kcal/mol. This is most likely due to the fact that model 1 has been
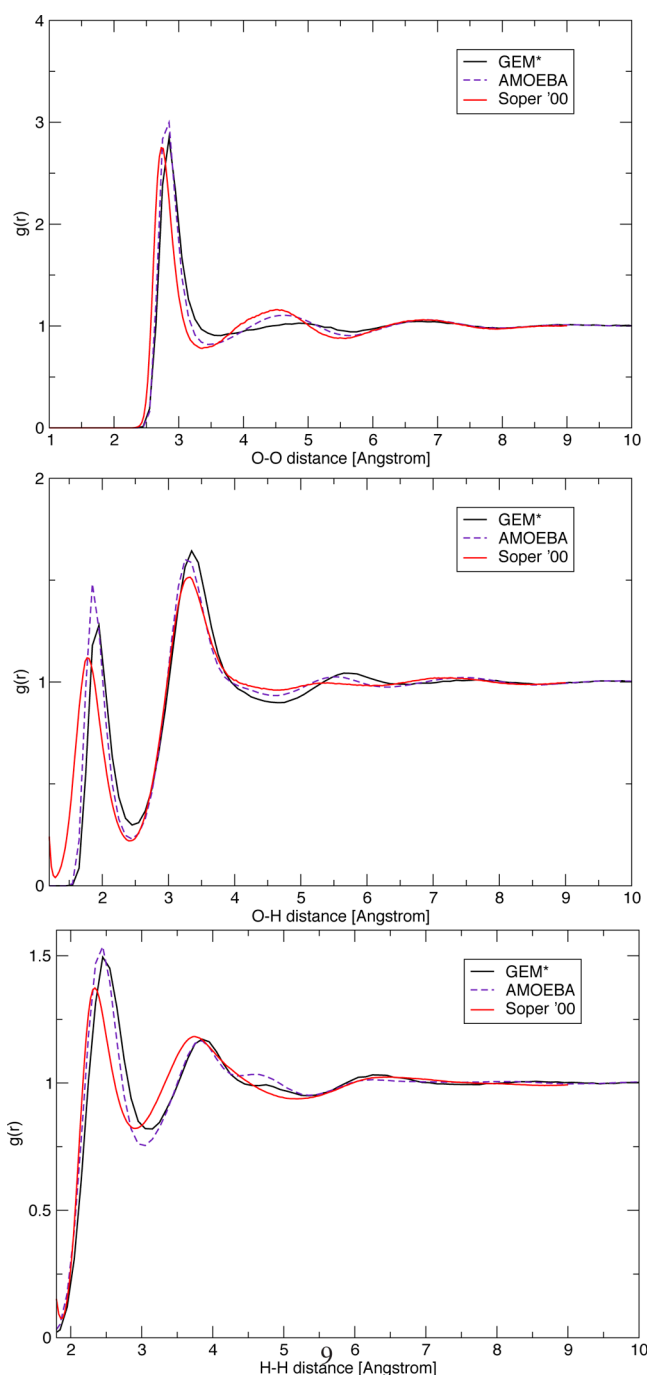
Figure 2. O−O (top), O−H (middle), and H−H (bottom) radial distribution functions. Soper '00 denotes the neutron scattering derived experimental curve from ref 69.

parametrized using an intermediate level of theory (MP2/aug-cc-pVTZ), with a very limited number of random oligomers to account for many-body effects and does not explicitly account for charge−transfer effects. Conversely, model 2 gives a better agreement with respect to experimental results, although the many-body effects in this model are poorly described. The implementation of the NPT ensemble as well as a parametrization using the Babin data set and a method to optimize VdW parameters that involves QM and experimental data[70] are currently under investigation. This is expected to result in better agreement with QM and experimental bulk property data.

In summary, we have developed and implemented a new force field, GEM*, involving molecular electronic densities by combining GEM and AMOEBA terms. GEM* was tested by developing three parameter sets for water based on QM data. Tests were performed for a series of water dimers, clusters, and boxes of varying sizes which showed that model 1 gives the best results with respect to QM. GEM* enables the simulation of periodic systems involving Gaussian functions by means of PME and FFP. In addition, for large number of basis functions, it is possible to perform part of the integrals in reciprocal space to reduce computational time. Overall, a considerable speedup of the approach is possible through code optimization for both the density and polarization contributions.[71] Finally, GEM* opens short-term perspectives toward full GEM MD simulations as gradients of the charge transfer contribution have been recently coded (manuscript in preparation).

■ ASSOCIATED CONTENT

ⓢ Supporting Information

Details on molecular electronic density fitting, GEM* functional form, fitting details, fitting coefficients, energy and force analysis for dimers, energy analysis for selected oligomers, and total energy for the 216 water box for the NVE simulation. This material is available free of charge via the Internet at http://pubs.acs.org.

■ AUTHOR INFORMATION

Corresponding Author
*E-mail: andres@chem.wayne.edu.

Notes

The authors declare no competing financial interest.

■ ACKNOWLEDGMENTS

■ REFERENCES

(1) Case, D. A.; Cheatham, T. E., III; Darden, T. A.; Gohlke, H.; Luo, R.; Merz, K. M., Jr.; Onufirev, A.; Simmerling, C.; Wang, B.; Woods, R. J. *J. Comput. Chem.* **2005**, *26*, 1668−1688.

(2) Jorgensen, W. L.; Tirado-Rives, J. *J. Comput. Chem.* **2005**, *26*, 1669−1700.

(3) van der Spoel, D.; Lindahl, E.; Hess, B.; Groenhoff, G.; Mark, A. E.; Berensen, H. J. C. *J. Comput. Chem.* **2005**, *26*, 1701−1718.

(4) Christen, M.; Hünenberger, P. H.; Bakowies, D.; Baron, R.; Brúgl, R.; Geerke, D. P.; Heinz, T. N.; Kastenholz, M. A.; Kräutler, V.; Oostenbrink, C.; Peter, C.; Trzesniak, D.; van Gunsteren, W. F. *J. Comput. Chem.* **2005**, *26*, 1719−1751.

(5) MacKerrell, A. D.; Jr.; Brooks, B.; Brooks, C. L., III; Roux, N. B.; Won, Y.; Karplus, M. In *CHARMM: The Energy Function and Its Parametrization with an Overview of the Program" in Encyclopedia of Computational Chemistry*; Schleyer, P., Ed.; John Wiley & Sons Ltd.: New York, 1998; pp 271−277.

(6) Salomon-Ferrer, R.; Case, D. A.; Walker, R. C. *Wiley Interdiscip. Rev.: Comput. Mol. Sci.* **2013**, *3*, 198−210.

(7) Stone, A. J. *The Theory of Intermolecular Forces*; Oxford University Press: Oxford, U.K., 2000.

(8) Hermida-Ramón, J. M.; Brdarski, S.; Karlström, G.; Berg, U. *J. Comput. Chem.* **2003**, *24*, 161−176.

(9) Gresh, N.; Cisneros, G. A.; Darden, T. A.; Piquemal, J.-P. *J. Chem. Theory Comput.* **2007**, *3*, 1960−1986.

(10) Ponder, J. W.; Wu, C.; Ren, P.; Pande, V. S.; Chodera, J. D.; Schnieders, M. J.; Haque, I.; Mobley, D. L.; Lambrecht, D. S.; DiStasio, R. A., Jr.; Head-Gordon, M.; Clark, G. N. I.; Johnson, M. E.; Head-Gordon, T. *J. Phys. Chem. B* **2010**, *114*, 2549−2564.

(11) Day, P. N.; Jensen, J. H.; Gordon, M. S.; Webb, S. P.; Stevens, W. J.; Krauss, M.; Garmer, D.; Basch, H.; Cohen, D. *J. Chem. Phys.* **1996**, *105*, 1968−1986.

(12) Xie, W.; Gao, J. *J. Chem. Theory Comput.* **2007**, *3*, 1890−1900.

(13) Xie, W.; Orozco, M.; Truhlar, D. G.; Gao, J. *J. Chem. Theory Comput.* **2009**, *5*, 459−467.

(14) Shaik, M. S.; Liem, S. Y.; Popelier, t. Paul L. A.″. P. j. . j. y. . . v. . . n. . . p. . . .,.

(15) Price, S. In *Reviews in Computational Chemistry*; Lipkowitz, K., Boyd, D. B., Eds.; VCH Publishers: New York, 1999; Vol. *14*.

(16) Popelier, P. *Atoms in Molecules: An Introduction*; Prentice Hall: Harlow, England, 2000.

(17) Kosov, D. S.; Popelier, P. L. A. *J. Phys. Chem. A* **2000**, *104*, 7339−7345.

(18) Popelier, P. L. A.; Joubert, L.; Kosov, D. S. *J. Phys. Chem. A* **2001**, *105*, 8254−8261.

(19) Popelier, P. L. A.; Kosov, D. S. *J. Chem. Phys.* **2001**, *114*, 6539−6547.

(20) Freitag, M. A.; Gordon, M. S.; Jensen, J. H.; Stevens, W. J. *J. Chem. Phys.* **2000**, *112*, 7300−7306.

(21) Kairys, V.; Jensen, J. H. *Chem. Phys. Lett.* **1999**, *315*, 140−144.

(22) Piquemal, J.-P.; Gresh, N.; Giessner-Prettre, C. *J. Phys. Chem. A* **2003**, *107*, 10353−10359.

(23) Cisneros, G. A.; Tholander, S. N.-I.; Parisel, O.; Darden, T. A.; Elking, D.; Perera, L.; Piquemal, J.-P. *Int. J. Quantum Chem.* **2008**, *108*, 1905−1912.

(24) Wang, B.; Truhlar, D. G. *J. Chem. Theory Comput.* **2010**, *6*, 3330−3342.

(25) Stone, A. J. *J. Phys. Chem. A* **2011**, *115*, 7017−7027.

(26) Wheatley, R. *Mol. Phys.* **2011**, *7*, 761−777.

(27) Gavezzotti, A. *J. Phys. Chem. B* **2002**, *106*, 4145−4154.

(28) Eckhardt, C. J.; Gavezzotti, A. *J. Phys. Chem. B* **2007**, *111*, 3430−3437.

(29) Volkov, A.; Coppens, P. *J. Comput. Chem.* **2004**, *25*, 921−934.

(30) Coppens, P.; Volkov, A. *Acta Crystallogr., Sect. A* **2004**, *60*, 357−364.

(31) Paricaud, P.; Predota, M.; Chialvo, A. A.; Cummings, P. T. *J. Chem. Phys.* **2005**, *122*, 244511.

(32) Giese, T. J.; Chen, H.; Dissanayake, T.; Giambasu, G. M.; Heldenbrand, H.; Huang, M.; Kuechler, E. R.; Lee, T.-S.; Panteva, M. T.; Radak, B. K.; York, D. M. *J. Chem. Theory Comput.* **2013**, *9*, 1417−1427.

(33) Hu, H.; Lu, Z.; Elstner, M.; Hermans, J.; Yang, W. *J. Phys. Chem. A* **2007**, *111*, 5685−5691.

(34) Cisneros, G. A.; Piquemal, J. P.; Darden, T. A. *J. Chem. Phys.* **2005**, *123*, 044109.

(35) Piquemal, J. P.; Cisneros, G. A.; Reinhardt, P.; Gresh, N.; Darden, T. A. *J. Chem. Phys.* **2006**, *124*, 104101.

(36) Cisneros, G. A.; Piquemal, J. P.; Darden, T. A. *J. Chem. Phys.* **2006**, *125*, 184101.

(37) Boys, S. F.; Shavit, I. In *A Fundamental Calculation of the Energy Surface for the System of Three Hydrogen Atoms*; WIS-AF-13, AD212985, NTIS: Springfield, VA, 1959.

(38) Dunlap, B. I.; Connolly, J. W. D.; Sabin, J. R. *J. Chem. Phys.* **1979**, *71*, 4993−4999.

(39) Köster, A. M.; Calaminici, P.; Gómez, Z.; Reveles, U. Density Functional Theory Calculation of Transition Metal Clusters. In *Reviews of Modern Quantum Chemistry, A Celebration of the Contribution of Robert G. Parr*; Sen, K., Ed.; World Scientific: Singapore, 2002; pp 1439−1475.

(40) Kitaura, K.; Morokuma, K. *Int. J. Quantum Chem.* **1976**, *10*, 325−340.

(41) Bagus, P. S.; Hermann, K.; Bauschlicher, C. W., Jr. *J. Chem. Phys.* **1984**, *80*, 4378−4386.

(42) Stevens, W. J.; Fink, W. H. *Chem. Phys. Lett.* **1987**, *139*, 15−22.

(43) Jeziorski, B.; Moszynski, R.; Szalewicz, K. *Chem. Rev.* **1994**, *94*, 1887−1930.

(44) Glendening, E. D. *J. Am. Chem. Soc.* **1994**, *118*, 2473−2482.

(45) Mo, Y.; Gao, J.; Peyerimhoff, S. D. *J. Chem. Phys.* **2000**, *112*, 5530−5538.

(46) Heßelmann, A.; Jansen, G.; Schütz, M. *J. Chem. Phys.* **2005**, *122*, 14103−14120.

(47) Piquemal, J.-P.; Marquez, A.; Parisel, O.; Giessner-Prettre, C. *J. Comput. Chem.* **2005**, *26*, 1052−1062.

(48) Khaliullin, R. Z.; Head-Gordon, M.; Bell, A. T. *J. Chem. Phys.* **2006**, *124*, 204105.

(49) Lu, Z.; Zhou, N.; Wu, Q.; Zhang, Y. *J. Chem. Theory Comput.* **2011**, *7*, 4038−4049.

(50) Cisneros, G. A.; Piquemal, J. P.; Darden, T. A. *J. Phys. Chem. B* **2006**, *110*, 11571−11581.

(51) Chaudret, R.; Ulmer, S.; van Severen, M.-C.; Gresh, N.; Parisel, O.; Cisneros, G. A.; Darden, T. A.; Piquemal, J.-P. *AIP Conf. Proc.* **2009**, *1102*, 185−192.

(52) Essmann, U.; Perera, L.; Berkowitz, M.; Darden, T. A.; Lee, H.; Pedersen, L. G. *J. Chem. Phys.* **1995**, *103*, 8577−8593.

(53) York, D.; Yang, W. *J. Chem. Phys.* **1994**, *101*, 3298−3300.

(54) Darden, T. A. Dual bases in crystallographic computing. In *International Tables of Chrystallography*; Shmueli, U., Ed.; Kluwer Academic Publishers: Dordrecht, The Netherlands, 2007; Vol. B.

(55) Ren, P.; Ponder, J. W. *J. Phys. Chem. B* **2003**, *107*, 5933−5947.

(56) Ren, P.; Ponder, J. W. *J. Comput. Chem.* **2002**, *23*, 1497−1506.

(57) Ren, P.; Wu, C.; Ponder, J. W. *J. Chem. Theory Comput.* **2011**, *7*, 3143−3161.

(58) Wheatley, R. J.; Price, S. L. *Mol. Phys.* **1990**, *69*, 507−533.

(59) Domene, C.; Fowler, P. W.; Wilson, M.; Madden, P.; Wheatley, R. J. *Chem. Phys. Lett.* **2001**, *333*, 403−412.

(60) Thole, B. *Chem. Phys.* **1981**, *59*, 341−350.

(61) Cisneros, G. A. *J. Chem. Theory Comput.* **2012**, *12*, 5072−5080.

(62) Andzelm, J.; Wimmer, E. *J. Chem. Phys.* **1992**, *96*, 1280−1303.

(63) Godbout, N.; Andzelm, J. *DGauss*, versions 2.0, 2.1, 2.3, 4.0; Computational Chemistry List, Ltd.: Columbus, OH, 1999. The file that contains the A1, A2, and P1 auxiliary basis sets can be obtained from the CCL WWW site at http://www.ccl.net/cca/data/basis-sets/DGauss/basis.v3.html.

(64) Stone, A. J. *J. Chem. Theory Comput.* **2005**, *1*, 1128−1132.

(65) Temelso, B.; Archer, K. A.; Shields, G. C. *J. Phys. Chem. A* **2011**, *115*, 12034−12046.

(66) Babin, V.; Medders, G. R.; Paesani, F. *J. Phys. Chem. Lett.* **2012**, *3*, 3765−3769.

(67) Babin, V.; Leforestier, C.; Paesani, F. *J. Chem. Theory Comput.* **2013**, *9*, 5395−5403.

(68) Ewald, P. *Ann. Phys.* **1921**, *64*, 253−287.

(69) Soper, A. *Chem. Phys.* **2000**, *258*, 121−137.

(70) Burger, S. K.; Cisneros, G. A. *J. Comput. Chem.* **2013**, *34*, 2313−2319.

(71) Lipparini, F.; Lagardère, L.; Stamm, B.; Cancès, E.; Schnieders, M.; Ren, P.; Maday, Y.; Piquemal, J. *J. Chem. Theory Comput.* **2014**, accepted; DOI: 10.1021/ct401096t.